

Supplementary Material

October 12, 2025

Contents

- Appendix A: Discussion on the relationship between CNN and Transformer in cross-attention
- Appendix B: Detailed regional classification method
- Appendix C: Analysis of the SEED-VII dataset
- Appendix D: Cross-validation on the SEED-IV dataset
- Appendix E: What happened when only one region?
- Appendix F: Experimental results on HBUED dataset with fewer electrodes

1 Appendix A: Discussion on the relationship between CNN and Transformer in cross-attention

The results in Table 1 indicate that the CNN branch not only contributes to the extraction of regional features, but also plays a greater role in conjunction with the Transformer branch, effectively integrating local and global features through cross-attention to enhance the representation of brain region features. However, we observed that removing the CNN only resulted in a 0.85% decrease in accuracy. This initially raised concerns about whether the CNN branch played a limited role. However, further investigation revealed that this phenomenon is primarily due to the residual connection within the cross-attention structure. In this appendix, we provide an in-depth analysis of the relationship between residual connection and feature contributions from the CNN and Transformer branches.

We observed the model structure and noticed that we introduced residual connection (one of the commonly used operations in Transformers) in the cross-attention structure, as shown in Formula (1).

$$F = MHA(F_{trans}, F_{cnn}, F_{cnn}) + F_{trans} \quad (1)$$

Table 1: The verification of the validity of the relevant modules of DFRNet on the SEED-IV dataset.

No structure	CNN	Transformer	Cross-attention	RFM	ACC / Std(%)	F1 / Std(%)
No CNN	✗	✓	✓	✓	84.43 / 13.42	80.89 / 16.70
No Transformer	✓	✗	✓	✓	80.32 / 13.75	76.59 / 16.53
No CNN branch	✗	✓	✗	✓	83.25 / 12.78	79.22 / 16.82
No Transformer branch	✓	✗	✗	✓	83.53 / 13.13	81.14 / 15.37
No cross-attention	✓	✓	✗	✓	83.95 / 13.10	80.24 / 16.82
No REM	✓	✓	✓	✗	82.79 / 14.38	79.51 / 17.07
Completed structure	✓	✓	✓	✓	85.28 / 14.01	81.81 / 17.24

A cross (✗) indicates that DFRNet does not contain the structure, while a check mark (✓) indicates that it does.

Here, F_{trans} represents the features from the Transformer branch, and F_{cnn} represents features from the CNN branch. The Multi-Head Attention (MHA) treats the Transformer features as the query (Q) and CNN features as the key and value (K and V). The result is then added back to the original Transformer features through a residual connection.

We speculate that the residual connection allows feature F to retain a significant amount of features from the Transformer branch after cross-attention. When CNN features are replaced by Transformer, the overall feature changes within the model are not particularly significant, and the model still learns relatively good content, resulting in only a 0.85% decrease. To validate our hypothesis, we conducted additional experiments by swapping the input positions of the CNN and Transformer branches in the cross-attention and repeating the ablation in Table 1. The experimental results are shown in Table 2. When the features from the CNN branch are used as Q, and the features from the Transformer branch are used as K and V, the accuracy is 81.74%. When we remove the Transformer, the result is 80.32%, a decrease of only 1.42%. Therefore, it is due to the existence of residual connection that replacing another input in cross-attention does not have as large an impact on overall features as initially imagined.

Table 2: The verification of the validity of the relevant modules of DFRNet on the SEED-IV dataset.

	Cross-attention	ACC / Std(%)	F1 / Std(%)
Swap the input	$F = MHA(F_{cnn}, F_{trans}, F_{trans}) + F_{cnn}$	81.74 / 11.83	78.87 / 13.63
No trans	$F = MHA(F_{cnn}, F_{cnn}, F_{cnn}) + F_{cnn}$	80.32 / 13.75	76.59 / 16.53
Original input	$F = MHA(F_{trans}, F_{cnn}, F_{cnn}) + F_{trans}$	85.28 / 14.01	81.81 / 17.24
No CNN	$F = MHA(F_{trans}, F_{trans}, F_{trans}) + F_{trans}$	84.43 / 13.42	80.89 / 16.70

We realize that two additional questions need to be explained here: “Why introduce residual connection in cross-attention?” This is because, in our preliminary experiments and model exploration, We found that introducing residual connection would yield better results. Furthermore, the self-attention mechanism in standard Transformers also includes this residual connection, so we incorporated it as well. Another question is, “Is the CNN branch necessary?” It is important to note that the results in Tables 1 and 2 are the average results from the three sessions of SEED-IV. After adding CNN, there was a stable improvement of 0.85% on average in

the dataset, which is still considerable. This indicates that the CNN structure plays a significant role.

Furthermore, by comparing the results of “No CNN” and “No Transformer” in Tables 1 and 2, we find that the Transformer branch is suitable for the cross-attention structure, while the features of the CNN branch may not be suitable for input into the cross-attention alone. We speculate that in our cross-attention structure, the fusion relationship between local features and global features is more likely to be the former supplementing and assisting the latter.

2 Appendix B: Detailed regional classification method

To make our research more complete, we added three brain region divisions as shown in Figure 1 to explore the impact of different brain region division methods on the accuracy of DRFNet.

(1) The detailed introduction to other three ways of brain region division:

First, we set up a non-overlapping brain region division, as shown in Figure 1 (a). This division retains the division of regions 1/2/4/7, while compressing regions 3/5/6, thereby preserving the original division as much as possible.

Second, we designed a brain region division similar to Yeo’s 7-network, as shown in Figure 1(b). Yeo et al. [1] conducted a large-scale resting-state functional connectivity study, performing data-driven clustering analysis on cortical surface data from 1,000 healthy young adults and dividing the brain into seven major functional networks at the coarsest resolution. Yeo’s 7-network achieved a consistency of up to 97.4% across different subsamples. Due to the inability to determine the exact electrode locations and the complexity of Yeo’s 7-network, we were unable to achieve complete alignment with its division; however, we have made every effort to align as closely as possible with this standard.

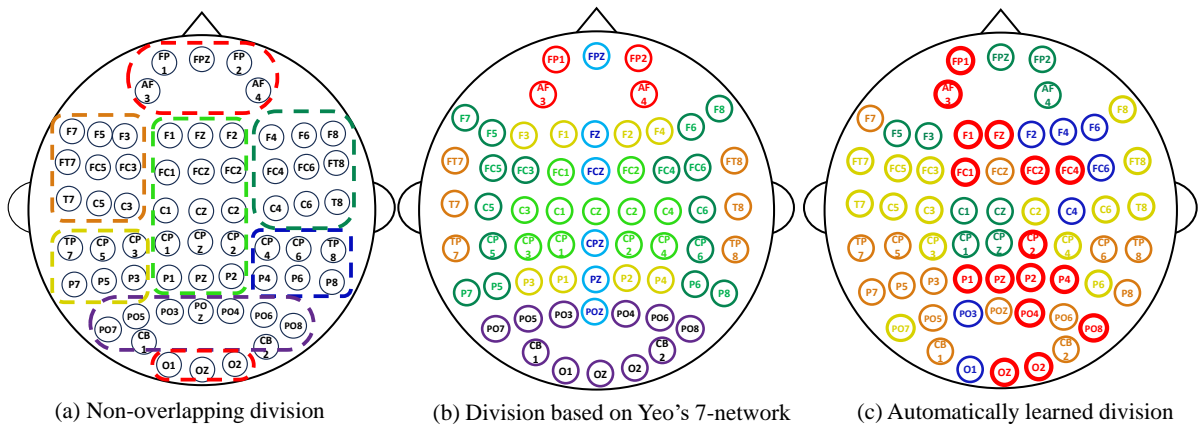


Figure 1: The division methods of the brain regions

At last, we adopted a data-driven brain region segmentation method called Automatically learned division. Previous studies have used GCN[2] methods to capture spatial information

between electrodes. A common single-layer GCN formula is shown below:

$$H^{l+1} = \sigma(\hat{D}^{-1/2} \hat{A} \hat{D}^{-1/2} H^l W^l) \quad (2)$$

where A is the adjacency matrix, $\hat{A} = A + I$, \hat{D} is the degree matrix of \hat{A} , H is the feature of the graph nodes, and W is the learnable parameter matrix. The GCN method utilizes an adjacency matrix to introduce “structural or functional” connections between electrodes into the feature aggregation and learning process, thereby enabling the neural network to capture the relationships between electrodes. Among them, RGNN[3] is a well-known GCN method in the field of EEG emotion recognition. However, it sets the adjacency matrix as learnable, and after feeding it with a large amount of data, the adjacency matrix A learns the potential, deep-level relationships between EEG electrodes.

The adjacency matrix reflects the correlations between electrodes, and we consider dividing the brain into regions based on the automatically learned A . Therefore, we replicated the RGNN method, using three session data to train the network on the SEED-IV dataset, and then weighted the adjacency matrices of 15 subjects based on the accuracy on the test set to obtain a comprehensive adjacency matrix A . For the obtained A , we first used thresholding to retain only the top 10% of the strongest edges, i.e., the most significant connections. The Leiden community detection algorithm [4] can partition nodes in a graph into several “communities,” ensuring that nodes within the same community are as closely connected as possible, while connections between different communities are as sparse as possible. Therefore, we used the Leiden algorithm to divide the brain into irregular regions as shown in Figure 1 (c). The code for this part has been made publicly available on GitHub to ensure the reproducibility of the experiment and facilitate communication among scholars. (https://github.com/braverSheep/DRFNet/tree/main/brain_region_division)

Table 3: The results of four different brain region divisions on the SEED and SEED-IV datasets.

Datasets	Fusion method	ACC (%)	Std (%)	F1-score (%)	Std (%)
SEED	Division based on Yeo’s 7-network	96.36	07.13	96.03	07.65
	Automatically learned division	93.84	08.85	93.36	09.46
	Non-overlapping division	94.66	08.55	94.18	09.08
	Original division	97.27	06.15	97.00	06.76
SEED-IV	Division based on Yeo’s 7-network	84.09	13.63	80.53	17.27
	Automatically learned division	82.54	13.72	79.16	16.86
	Non-overlapping division	83.83	12.44	82.19	14.91
	Original division	85.28	14.01	81.81	17.24

(2) The analysis of experimental results:

Table 3 shows the results of the four brain region partitioning methods on the SEED and

SEED-IV datasets. Based on the experimental results, we can summarize the following points:

1. The original brain region segmentation method is more suitable for our approach.
2. Our model still achieves acceptable results under Yeo’s 7-network brain region segmentation method, indicating that the model has a certain degree of robustness for brain regions.
3. Under the original division method, the accuracy of non overlapping is lower, which may be because the non overlapping method deprives electrodes located at the edge of brain regions of the ability to exchange information in multiple areas.
4. As can be clearly seen from the table, the accuracy of the Automatically learned division method has significantly decreased on both the SEED and SEED-IV datasets. First, this indicates that DRFNet is not without requirements for brain region division; the more reasonable the brain region division, the better DRFNet can perform. Second, it reflects that there are certain difficulties in automatically dividing brain regions through data, and we speculate that this may be more influenced by issues such as insufficient data volume and poor data quality. The actual situation needs to be verified through more experiments, and we plan to explore this as one of our next research directions.

3 Appendix C: Analysis of the SEED-VII dataset

Compared to other datasets, DRFNet’s performance on SEED-VII has declined significantly. SEED-VII is the latest emotion dataset released by Shanghai Jiao Tong University’s Brain-like Computing and Machine Intelligence research group. As shown in the Figure 2, the overall accuracy of the models reported by them on this dataset is not high. Most models perform poorly, which in turn suggests that this is likely due to the complexity of the categories and the characteristics of the dataset itself.

The accuracies and F1 scores (Avg./Std., %) achieved by different methods using EEG or eye movement signals.

Method	EEG signals						Eye movements
	delta band	theta band	alpha band	beta band	gamma band	all bands	
Accuracy	KNN [70]	28.21/5.76	28.47/7.02	31.92/6.51	34.83/5.77	37.20/6.06	36.43/5.38
	HCNN [36]	42.33/6.36	42.63/5.28	43.62/4.82	47.79/6.77	48.18/6.10	52.42/6.47
	RGNN [37]	42.31/5.14	41.73/5.53	43.93/4.98	44.68/5.51	45.49/4.73	48.50/6.83
	Transformer [42]	46.87/4.10	47.01/4.23	48.78/5.39	53.10/6.34	53.96/6.60	56.04/7.82
	GCNCA [38]	49.97/4.94	50.46/4.29	53.26/5.45	58.36/6.69	59.50/5.77	58.04/7.78
	MAET	-	-	-	-	-	58.11/8.78
F1 score	KNN [70]	26.00/5.98	26.12/7.25	29.67/6.64	33.22/5.59	34.98/5.62	34.08/5.79
	HCNN [36]	37.85/7.78	38.30/5.72	39.66/5.23	44.05/7.55	44.33/6.68	49.02/6.80
	RGNN [37]	37.85/5.56	36.13/5.79	39.18/5.43	40.68/06.61	41.77/5.50	45.32/7.20
	Transformer [42]	43.20/4.26	43.85/4.74	45.48/5.23	49.81/6.70	51.48/6.96	53.35/8.30
	GCNCA [38]	47.61/5.14	47.92/5.01	50.99/5.71	55.97/7.12	57.54/5.90	55.48/8.30
	MAET	-	-	-	-	-	54.98/9.45

Figure 2: The performance results of various models reported in the original paper[5] on the SEED-VII dataset.

First, increasing the number of emotion categories will greatly reduce the spatial intervals between various emotion signals, making it difficult for the model to distinguish between similar

emotion categories. As shown in Figure 3, DRFNet misclassified a large number of happy and fearful samples as surprised, because happiness, fear, and surprise all belong to high arousal states. Additionally, sadness is typically characterized by low arousal and negative valence. If the sadness is not sufficiently intense, and the participant is in a “mild sadness” state, EEG signals may resemble neutral states. As shown in the confusion matrix, DRFNet incorrectly classified sadness samples as neutral emotions.

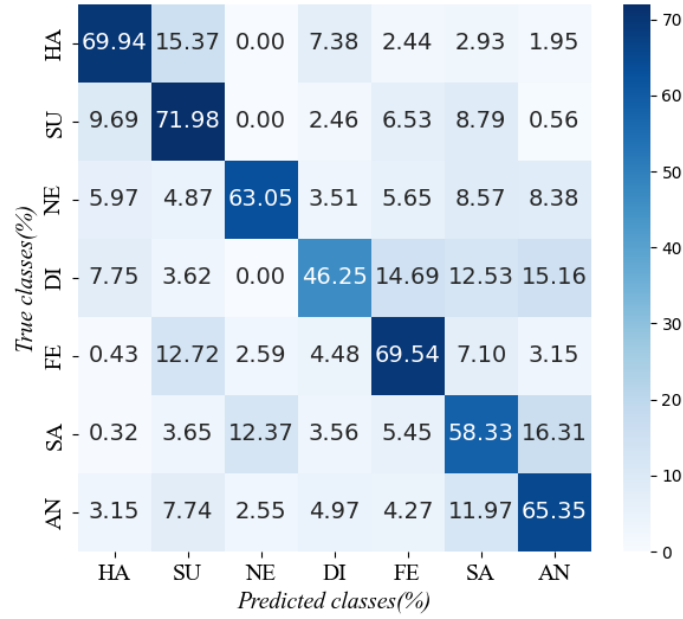


Figure 3: Confusion matrix of DRFNet’s results on the SEED-VII dataset.

Secondly, when collecting data, if the participants cannot be effectively stimulated to produce the corresponding emotions, the quality of the data will be low. As shown in the Figure 4, this is the "subjectID_date_sessionID_save_info.csv" file included with the publicly available SEED-VII, which contains the feedback from subject 1 for each movie clip. From this, we can see that some trials failed to effectively trigger the participants to produce the corresponding emotions, with many participants rating their level of successful induction below 0.5 (on a scale from 0 to 1). The SEED-VII data may contain a significant number of false labels, making it quite challenging.

Index	Task	Movie Clip	Rating
1	emotion tasks	movie\七类\happy\5钱学森2.mp4	0.3
2	emotion tasks	movie\七类\neutral\Suzhou 1.m4v	0.1
3	emotion tasks	movie\七类\disgust\9.11.mp4	0.6
4	emotion tasks	movie\七类\sad\5你是我的生命2.mp4	0.1
5	emotion tasks	movie\七类\anger\8.mp4	0.6
6	emotion tasks	movie\七类\anger\6.mp4	0.5
7	emotion tasks	movie\七类\disgust\4养父2.mp4	0.2
8	emotion tasks	movie\七类\disgust\9.mp4	0.9
9	emotion tasks	movie\七类\neutral\Lijiang 1.m4v	0
10	emotion tasks	movie\七类\happy\4被偷走的那五年.mp4	0
11	emotion tasks	movie\七类\happy\2那些年.mp4	0.1
12	emotion tasks	movie\七类\neutral\IDE接口修复.mp4	0
13	emotion tasks	movie\七类\disgust\9.33.mp4	0.7
14	emotion tasks	movie\七类\disgust\2山核桃之恋-老三去世-加长版.mp4	0.2
15	emotion tasks	movie\七类\anger\3.mp4	0.5
16	emotion tasks	movie\七类\anger\2.mp4	0.9
17	emotion tasks	movie\七类\sad\1唐山大地震-救弟弟-加长版.mp4	0.9
18	emotion tasks	movie\七类\disgust\6.39.mp4	0.7
19	emotion tasks	movie\七类\neutral\Huangshan 1.m4v	0.1
20	emotion tasks	movie\七类\happy\1宝贝计划1.mp4	0.6

Index	Task	Movie Clip	Rating
1	emotion tasks	movie\七类\disgust\53.mp4	1
2	emotion tasks	movie\七类\disgust\非常有毒.mp4	0.6
3	emotion tasks	movie\七类\disgust\笔仙3.1.mp4	0.6
4	emotion tasks	movie\七类\surprise\Surprise 9.mp4	0.6
5	emotion tasks	movie\七类\happy\重返20岁2.mp4	0.7
6	emotion tasks	movie\七类\happy\山楂树之恋-骑车.mp4	0.6
7	emotion tasks	movie\七类\surprise\Surprise 8.mp4	0.6
8	emotion tasks	movie\七类\disgust\1.mp4	0.4
9	emotion tasks	movie\七类\disgust\致青春-分手.mp4	0.6
10	emotion tasks	movie\七类\disgust\44.mp4	0.7
11	emotion tasks	movie\七类\disgust\39.mp4	0.7
12	emotion tasks	movie\七类\disgust\养父4.mp4	0.6
13	emotion tasks	movie\七类\disgust\Annabelle.mp4	0.7
14	emotion tasks	movie\七类\surprise\Surprise 4.mp4	0.9
15	emotion tasks	movie\七类\happy\听说-真相大白.mp4	0.7
16	emotion tasks	movie\七类\happy\9再见金华站-1.mp4	0.3
17	emotion tasks	movie\七类\surprise\surprise 12.mp4	0.8
18	emotion tasks	movie\七类\disgust\8蓝兰神功7.mp4	0.5
19	emotion tasks	movie\七类\disgust\亲爱的9.mp4	0.6
20	emotion tasks	movie\七类\disgust\35.mp4	0.8

Figure 4: Confusion matrix of our model results on the SEED-VII dataset.

4 Appendix D: Cross-validation on the SEED-IV dataset

To facilitate fair future comparisons and provide a reproducible benchmark, we supplement our work with a subject-dependent k-fold cross-validation evaluation on the SEED-IV dataset. This complements the main experimental setup based on commonly used fixed splits in the literature and serves as a reference for future researchers interested in robust evaluation under multiple splits.

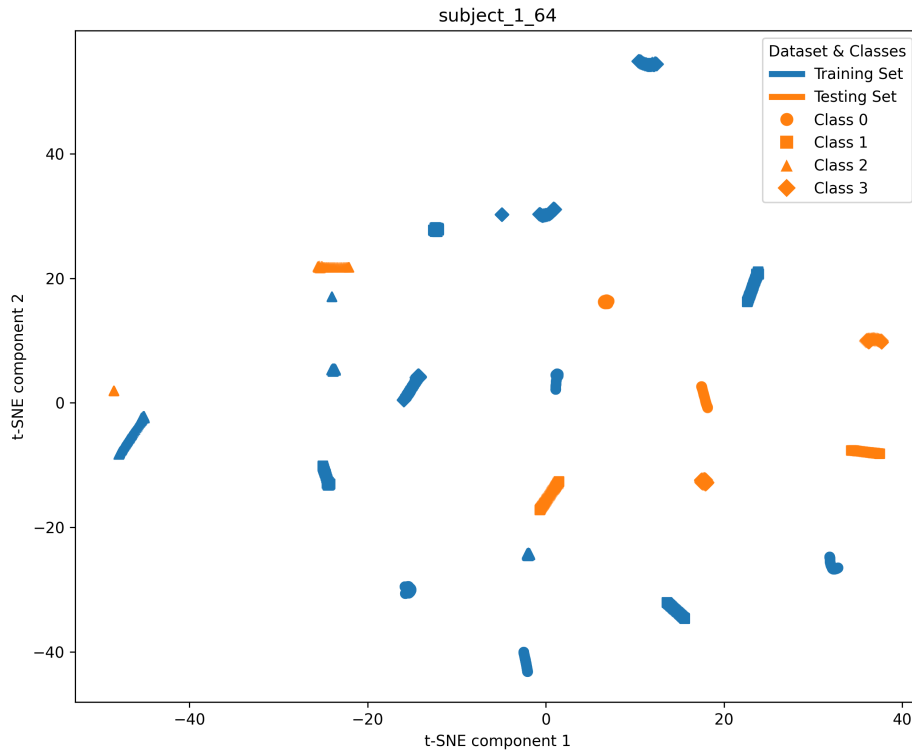


Figure 5: t-SNE visualization of subject1 data in the SEED dataset. There are a total of 24 data clusters, corresponding to the 24 trial experiments collected for subject 1.

While existing works such as DGCNN[6], RGNN[3], and PGCN[7] typically follow subject-dependent evaluation protocols with fixed training/test trials per subject, some studies have employed n-fold cross-validation. However, we have not yet seen a unified cross-validation method. In particular, certain cross-validation methods divide EEG samples randomly without preserving trial integrity, which may lead to data leakage—samples from the same trial appearing in both training and test sets—thus overestimating performance. As shown in Figure 5, samples from the same trail are highly similar. We have conducted experiments in which all data were randomly divided into n folds, which makes the final experimental results easily approach 1. Therefore, samples from the same trial should not be separated, as this could potentially lead

to label leakage. To avoid this issue, we adopt a trial-level fold splitting strategy: in each fold, entire trials are kept intact and not split between training and test sets.

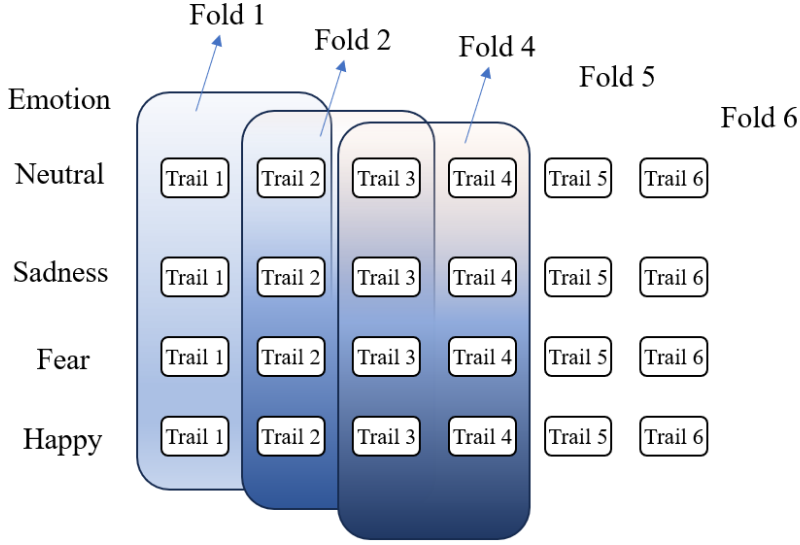


Figure 6: 6-fold cross-validation on the SEED-IV dataset. In the SEED-IV dataset, each person has 24 trial data points, with 6 trials for each emotion category.

Table 4: Fold-wise ACC and Std for Each Session, Their Three-Session Averages, and Overall Averages. (%)

fold	session1		session2		session3		Average of 3 sessions		All averages	
	ACC	Std	ACC	Std	ACC	Std	ACC	Std	ACC	Std
1	78.42	12.51	86.77	10.16	89.39	9.79	84.86	10.82	87.12	11.41
2	80.48	12.11	86.13	8.24	90.00	8.72	85.53	9.69		
3	87.29	10.32	91.76	8.40	91.81	7.71	90.28	8.81		
4	86.67	12.82	84.59	12.51	91.22	13.15	87.49	12.82		
5	83.13	14.54	83.75	13.55	84.24	16.64	83.70	14.91		
6	83.19	12.46	86.60	10.57	89.33	11.20	86.37	11.41		

For the convenience of future researchers who wish to use cross-validation to fairly compare our model, we will supplement our experiments with cross-validation and publish the fold division method and results on GitHub (https://github.com/braverSheep/DRFNet/tree/main/SEED-IV_cross_validation). We have temporarily conducted cross-validation on the SEED-IV dataset, following the original test set splitting ratio, where two trials per emotion are used as the test set. The data is then split into 6 folds as shown in the Figure 6. Table 4 presents our experimental results on the SEED-IV dataset.

The average accuracy across all folds and sessions is 87.12%, demonstrating strong and stable performance of DRFNet under multi-fold subject-dependent settings. We plan to extend this cross-validation framework to other datasets (e.g., SEED, SEED-V) and make all fold splits publicly available to promote fairness and reproducibility in EEG emotion recognition research.

5 Appendix E: What happened when only one region?

In the main content of the manuscript, we conduct ablation experiments on brain regions and find that the regions in the bilateral temporal lobes possess more information related to emotions. However, previous experiments are all based on results from multiple brain regions. We are curious about emotion recognition in individual brain regions. Therefore, we conduct experiments on individual brain regions using the SEED, SEED-IV, and SEED-V datasets, and the results are shown in Table 5.

Table 5: The verification of the importance of brain regions in datasets SEED, SEED-IV, and SEED-V.

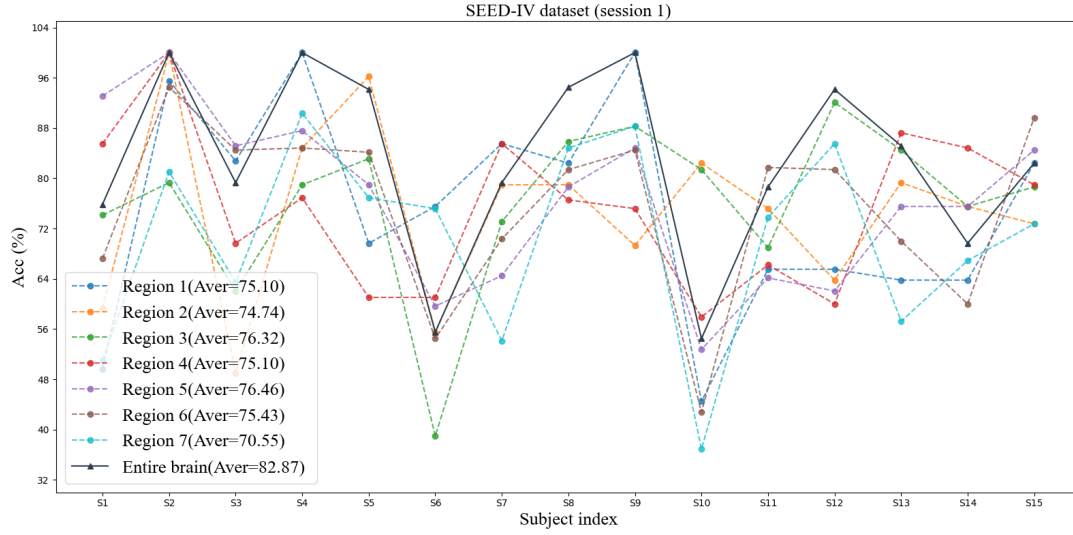
Removed regions	SEED (ACC/Std %)	SEED-IV (ACC/Std %)	SEED-V (ACC/Std %)
Only region 1	82.68 / 15.87	78.81 / 15.13	74.21 / 17.26
Only region 2	87.49 / 12.54	76.46 / 14.24	70.07 / 16.93
Only region 3	88.90 / 13.98	78.46 / 12.97	73.06 / 17.08
Only region 4	90.23 / 11.88	75.68 / 14.85	72.13 / 17.33
Only region 5	88.34 / 12.67	76.86 / 14.33	71.54 / 16.69
Only region 6	87.11 / 11.34	79.06 / 13.02	73.43 / 16.57
Only region 7	78.08 / 15.34	73.64 / 14.51	68.45 / 15.64
Seven regions	97.27 / 06.15	85.28 / 14.01	83.73 / 14.67

It is evident from the table that the performance of emotion recognition based on data from a single brain region is significantly worse than when using data from the entire brain. For instance, when using data from region 7, accuracies of 78.08%, 73.64%, and 68.45% are achieved on SEED, SEED-IV, and SEED-V, respectively, which are 19%, 18%, and 15% lower than when using all data. Additionally, it can be observed that the accuracies for the temporal lobe regions (Regions 2/3/4/5) are slightly higher, which corroborates the experimental results presented in the manuscript.

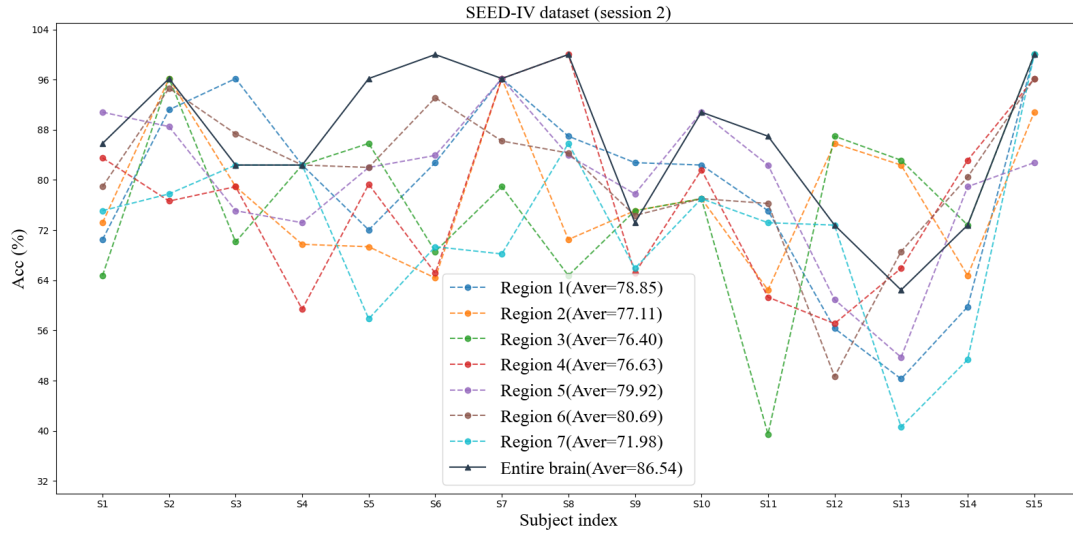
Table 5 presents a comparison between individual regions and the entire brain at the average level. Conversely, we would like a more detailed comparison. Therefore, we have included Figure 7, which displays the results obtained using data from individual brain regions across three sessions of SEED-IV.

Although the accuracy of emotion recognition using data from the entire brain is significantly higher on average than that using data from a single brain region, surprisingly, we find that, when specific to a particular subject, the accuracy achieved in local brain regions may actually be higher. This point can be demonstrated in Figure 7. In the presentation of results from three sessions, there are individuals whose prediction accuracy using data from a single brain region is higher than using all data, such as subjects 1/3/5/6/7/10/11/13/14/15 in session 1. This phenomenon accounts for a non-negligible proportion.

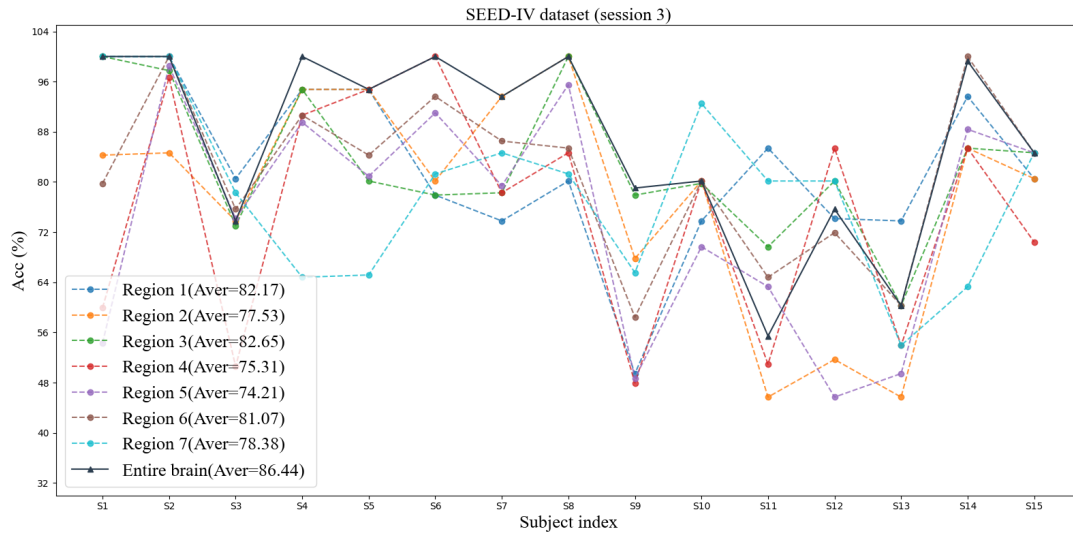
We believe this reflects at least two issues:



(a) Session 1



(b) Session 2



(c) Session 3

Figure 7: Detailed experimental results using individual brain regions on the SEED-IV dataset.

(1) There are still limitations with our method. The DRFNet can adaptively focus on the features of important brain regions, as evident in the sub-graphs of sessions 2 and 3 in Figure 7, which indeed show that it pays attention to the features of key regions and achieves the highest accuracy in most cases. However, there are still exceptions, indicating that DRFNet’s ability to focus on key brain regions has certain limitations, and the model still has room for improvement.

(2) The pure self-attention mechanism, based on data-driven, heavily relies on the quantity and quality of data. This represents one of the limitations of the attention mechanism. Perhaps we can introduce other methods to assist data-driven learning, thereby enhancing the model’s ability to focus on key brain regions.

The above findings provide inspiration for our next step of work.

6 Experimental results on HBUED dataset with fewer electrodes

Our DRFNet method was initially designed in the context of collecting EEG signals with 62 electrodes, and electrodes-to-region mapping was performed on this basis. In the manuscript, we conducted extensive experiments on four datasets (SEED, SEED-IV, SEED-V, SEED-VII), each containing data from multiple sessions. Given the number of datasets and the volume of data, the experimental results sufficiently demonstrate the effectiveness of the DRFNet.

However, we were curious about how DRFNet would perform on a dataset with fewer channels. Therefore, we conducted some experiments on the Hebei University Emotional EEG Dataset (HBUED) [8]. This dataset was collected from approximately 20 healthy subjects using a 32-channel EEG device with a sampling rate of 1000 Hz. During the experiment, emotional responses were elicited from the subjects by presenting videos as stimuli. After each stimulus, the subjects were asked to subjectively rate their emotional state using a self-assessment scale. Each trial corresponded to one emotional stimulus and included multi-channel EEG signals along with their corresponding valence and arousal labels.

We followed the experimental setup of HBUED[8] and conducted subject-dependent experiments on valence, arousal, and four-class classification using ten-fold cross-validation. The experimental results are presented in the Table 6. In addition, HBUED uses the same electrode positions as SEED data, except for only 32 electrodes. We still use 62 channels for data input processing, but for the remaining 30 channels without data, we fill them with a value of 0.

The performance of our proposed DRFNet on this dataset is significantly weaker compared to its performance on the 62-channel dataset, achieving only about 77% accuracy in both Valence and Arousal dimensions, and 65.71% in the four-class classification task, which is notably lower than DGCNN and RGNN. This indicates that DRFNet’s advantages are not as pronounced with low-channel EEG data. Furthermore, when the CNN branch is removed, the model’s performance only experiences a slight decline across all tasks, which also reflects that the benefits of local feature extraction are limited in the context of 32-channel scenarios.

Table 6: Classification accuracy on the HBUED dataset(acc/std %).

Method	Valence	Arousal	Four-class
SVM	63.67 / 08.70	64.21 / 08.62	52.32 / 11.23
Random forest	71.65 / 05.40	71.86 / 05.65	65.44 / 08.85
EEGNet [9]	77.09 / 08.01	76.65 / 06.53	60.57 / 08.86
SparseDGCNN [10]	85.96 / 04.54	85.52 / 04.33	70.23 / 05.94
DGCNN [6]	87.32 / 05.17	86.33 / 05.49	78.66 / 09.03
RGNN [3]	87.18 / 05.24	87.33 / 05.50	71.27 / 08.55
Ours	77.56 / 06.65	77.87 / 07.13	65.71 / 09.70
Ours (No CNN branch)	77.53 / 07.07	77.47 / 06.39	63.08 / 02.67

We believe this performance gap is closely related to the limited number of data acquisition channels. DRFNet was originally designed for 62-channel EEG data, leveraging regional segmentation and local-global feature fusion to fully utilize spatial structural information of brain regions. However, when the channel count drops to 32, the precision of regional segmentation and the ability to model brain region relationships are compromised, leading to reduced feature extraction capabilities. Additionally, fewer channels may also diminish the effectiveness of the regional attention mechanism, making it difficult for the model to fully demonstrate its advantages in high-density electrode scenarios.

In summary, although DRFNet performs well on high channel EEG datasets, there is still room for improvement in its performance on low channel EEG datasets. This also suggests that in future work, we need to design more suitable region partitioning and feature modeling mechanisms for low channel EEG signals to enhance the generality and robustness of the model.

References

- [1] B. Thomas Yeo, F. M. Krienen, J. Sepulcre, M. R. Sabuncu, D. Lashkari, M. Hollinshead, J. L. Roffman, J. W. Smoller, L. Zöllei, J. R. Polimeni *et al.*, “The organization of the human cerebral cortex estimated by intrinsic functional connectivity,” *Journal of neurophysiology*, vol. 106, no. 3, pp. 1125–1165, 2011.
- [2] T. N. Kipf and M. Welling, “Semi-supervised classification with graph convolutional networks,” *arXiv preprint arXiv:1609.02907*, 2016.
- [3] P. Zhong, D. Wang, and C. Miao, “Eeg-based emotion recognition using regularized graph neural networks,” *IEEE Transactions on Affective Computing*, vol. 13, no. 3, pp. 1290–1301, 2022.
- [4] V. A. Traag, L. Waltman, and N. J. Van Eck, “From louvain to leiden: guaranteeing well-connected communities,” *Scientific reports*, vol. 9, no. 1, pp. 1–12, 2019.
- [5] W.-B. Jiang, X.-H. Liu, W.-L. Zheng, and B.-L. Lu, “Seed-vii: A multimodal dataset of six basic emotions with continuous labels for emotion recognition,” *IEEE Transactions on Affective Computing*, pp. 1–16, 2024.

- [6] T. Song, W. Zheng, P. Song, and Z. Cui, “Eeg emotion recognition using dynamical graph convolutional neural networks,” *IEEE Transactions on Affective Computing*, vol. 11, no. 3, pp. 532–541, 2020.
- [7] M. Jin, C. Du, H. He, T. Cai, and J. Li, “Pgcn: Pyramidal graph convolutional network for eeg emotion recognition,” *IEEE Transactions on Multimedia*, 2024.
- [8] S. Liu, X. Wang, Y. An, Z. Wang, Z. Gu, Y. Zhang, and S. Zhao, “Hbued: An eeg dataset for emotion recognition,” *Journal of Affective Disorders*, p. 119397, 2025.
- [9] V. J. Lawhern, A. J. Solon, N. R. Waytowich, S. M. Gordon, C. P. Hung, and B. J. Lance, “Eegnet: a compact convolutional neural network for eeg-based brain–computer interfaces,” *Journal of neural engineering*, vol. 15, no. 5, p. 056013, 2018.
- [10] G. Zhang, M. Yu, Y.-J. Liu, G. Zhao, D. Zhang, and W. Zheng, “Sparsedgcnn: Recognizing emotion from multichannel eeg signals,” *IEEE Transactions on Affective Computing*, vol. 14, no. 1, pp. 537–548, 2021.